

## ELEMENTARY PARTICLES AND FIELDS

### Experiment

# Geophysical Aspect of Cosmic Ray Studies at the Tien Shan Mountain Station: Monitoring of Radiation Background, Investigation of Atmospheric Electricity Phenomena in Thunderclouds, and the Search for the Earthquake Precursor Effects

A. Shepetov<sup>1)\*</sup>, O. Kryakunova<sup>2)</sup>, S. Mamina<sup>1)</sup>, V. Ryabov<sup>1)</sup>, N. Saduyev<sup>3)</sup>,  
T. Sadykov<sup>4)</sup>, N. Salikhov<sup>2)</sup>, L. Vildanova<sup>1)</sup>, and V. Zhukov<sup>1)</sup>

Received July 12, 2021; revised July 12, 2021; accepted July 12, 2021

**Abstract**—The multipurpose detector complex of the Tien Shan mountain station of LPI provides the means to carry out studies in the various fields of experimental geophysics. The detectors of cosmic ray particles present at the station can be used for continuous monitoring of different types of background radiation: of the current flux of (1–100) GeV cosmic ray hadrons, of thermal neutrons in the surrounding environment, and of the gamma-rays with energy (30–3000) keV. Special system of the high altitude detectors permits to register the electrons accelerated up to several tens and hundreds of MeV by the atmospheric electric fields in thunderclouds, as well as the gamma radiation generated by these particles. A combination of diverse radiation receivers can be used for simultaneous detection of the time profiles of lightning emission in the different wave ranges of electromagnetic spectrum, starting from near ultraviolet and up to (1–30) MHz radio-waves, as well as of the electromagnetic pulses propagating over the global earth-ionosphere waveguide in the VLF, (1–10) kHz, and SLF, (1–10) Hz, frequency ranges. An underground complex of the neutron, gamma-ray, and acoustic detectors placed in a borehole at an up to ~300-m depth below the surface of the ground is used for detection of the various signals of geophysical origin, including those which could be triggered by interaction of penetrative cosmic ray particles with the matter of the earth's crust. Perspectives of geophysical experiments at the Tien Shan station are discussed here together with application opportunity of their results to various problems of the space physics, of the physics of atmospheric discharge and lightning development, of environmental monitoring, and of the monitoring of seismic processes for the purpose of timely earthquake forecast.

**DOI:** 10.1134/S1063778821130330

## 1. INTRODUCTION

As result of a step-by-step development of the experimental complex which lasted over decades at the Tien Shan mountain scientific station of the P.N. Lebedev Physical Institute [1, 2], a possibility has been now achieved to obtain experimental information which is of interest for many topical problems of modern geophysics, physics of atmospheric electricity, physics of the Sun and solar—terrestrial connections. The list of the studies presently carried out at the station includes the following subjects:

1. Continuous, over duration of many years, monitoring of the intensity of (1–100) GeV cosmic rays, that is, of the particles whose propagation is most influenced by the processes taking place at the Sun and in the interplanetary space [3]. Prolonged series of such measurements is necessary to construct the models of solar activity and of the heliosphere, to study various aspects of solar—terrestrial relations, to predict the geomagnetic situation and radiation level in the near-Earth space.
2. Similar direction of experimental activity at the Tien Shan station includes continuous measurements of the flux of thermal neutrons and of the (30–3000) keV gamma-rays in surrounding environment by the means of detectors installed in a number of points at the territory of the station [4]. The result of such monitoring may be useful for many urgent issues

<sup>1)</sup>Lebedev Physical Institute of the Russian Academy of Sciences (LPI), Moscow, 119991 Russia.

<sup>2)</sup>Institute of Ionosphere, Kamenskoe plato, Almaty, 050020 Kazakhstan.

<sup>3)</sup>Al-Farabi Kazakh National University, Institute of Experimental and Theoretical Physics, Almaty, 050040 Kazakhstan.

<sup>4)</sup>Satbayev University, Institute of Physics and Technology, Almaty, 050032 Kazakhstan.

\*E-mail: [ashep@tien-shan.org](mailto:ashep@tien-shan.org)

of ecological research, including the problem of global warming.

3. Detection of the different types of radiation which arise under the influence of strong electric field in thunderclouds: the streams of accelerated electrons and gamma-rays [2, 5–11], short-time neutron bursts in the moment of close lightning discharges [12, 13], electromagnetic emission of lightning in the various wave ranges [14, 15]. In particular, a possibility has been realized presently at the Tien Shan station to carry out direct registration of radiation fluxes in the spatial vicinity of electric discharge in thundercloud, at a distance of  $\sim(50\text{--}100)$  m only from the lightning core [16]. Such information is necessary for understanding the mechanism of lightning development which remains rather obscure up to the present time.
4. Multi-component monitoring of a variety of heterogeneous geophysical parameters, such as the characteristics of the global ionospheric waveguide, intensity of telluric currents, background level of hard radiations, intensity of the electromagnetic and acoustic emission signals deeply under the earth's surface. The main purpose of these measurements is to use collected data for the prognosis of seismic activity and earthquake forecasting in the seismically hazardous region which surrounds the Tien Shan mountain station [17, 18].

The information from all detectors of the Tien Shan station is in real time accumulated in a single database [19]. The latter is publicly accessible through the Internet for processing the archived data by participants of the third-party research groups.

## 2. MONITORING OF RADIATION BACKGROUND

Current intensity of the flux of  $(1\text{--}100)$  GeV cosmic rays at the Tien Shan station is measured using a NM64 type neutron supermonitor of standard design [20, 21]. Hitting the monitor, the cosmic ray hadrons with energies above 1 GeV cause generation of evaporation neutrons by interaction with target nuclei of a massive absorber which is a part of the installation. The neutrons generated in absorber can be detected by the gas-discharge proportional counters with a special gas filling which makes them sensitive to the thermal neutrons (the gas  $\text{BF}_3$  enriched with  $^{10}\text{B}$  isotope). Continuous recording of signal numbers received from these counters during successive time intervals with fixed duration (1 min) is

thus a means for precision monitoring of the intensity of hadronic component of cosmic rays.

The neutron monitor of the Tien Shan mountain station includes three  $(3 \times 2)$  m<sup>2</sup> units each of which contains six large neutron counters with dimensions  $(\varnothing 0.15 \times 2)$  m<sup>2</sup>.

An example of monitoring record of the cosmic ray intensity made at the Tien Shan NM64 supermonitor is presented in the upper plot of Fig. 1. This plot demonstrates a sharp recession of the cosmic ray flux (Forbush effect) which happened around the date of September 8, 2017 when the Earth was traversing a disturbance region of the interplanetary magnetic field caused by a solar flare. Together with the Forbush decrease, the diurnal and 27-days variations can be traced among the intensity of cosmic rays, which correspond to the effects of the Earth and Sun rotation.

For measurement the intensity of radiation background in the surrounding environment of the Tien Shan station several groups of gamma- and neutron detectors were installed in the three points at the station territory, such that the distance between them would be of about  $(100\text{--}200)$  m. The neutron detector in each point consists of a set of 12 neutron sensitive counters with the sizes  $(\varnothing 0.03 \times 1)$  m<sup>2</sup>. In contrast to the monitor, the neutron counters used for the measurement of neutron background do not have any internal absorber for hadronic interactions, and detect the thermalized neutrons which come directly from the outer environment. The gamma-detectors used in the monitoring points of radiation background are based on the crystals of inorganic NaI(Tl) scintillator. Effective area of a sensitive element in each detector is 560 m<sup>2</sup>, and it ensures registration of the flux of hard radiation simultaneously in 12 energy channels, starting from 30 keV and up to  $(3\text{--}5)$  MeV.

Example records of the counting rate intensity in the detectors of background radiations are shown in the middle and bottom plots of Fig. 1. The measurements presented here were made during a week in September 2019. A drop of neutron intensity seen in the middle plot since the date of 9 September reflects emergence of snow blanket at the Tien Shan station in those days, which induced a rise of neutron absorption because of the presence of surplus amount of hydrogen-rich material (water) in the environment. Numerous enhancements of gamma radiation with characteristic duration of  $(2\text{--}3)$  h in the bottom plot correspond to the periods of intensive precipitations commonly accompanied by the growth of local radiation background because of fallout of radioactive admixtures from the atmosphere together with the rainwater.

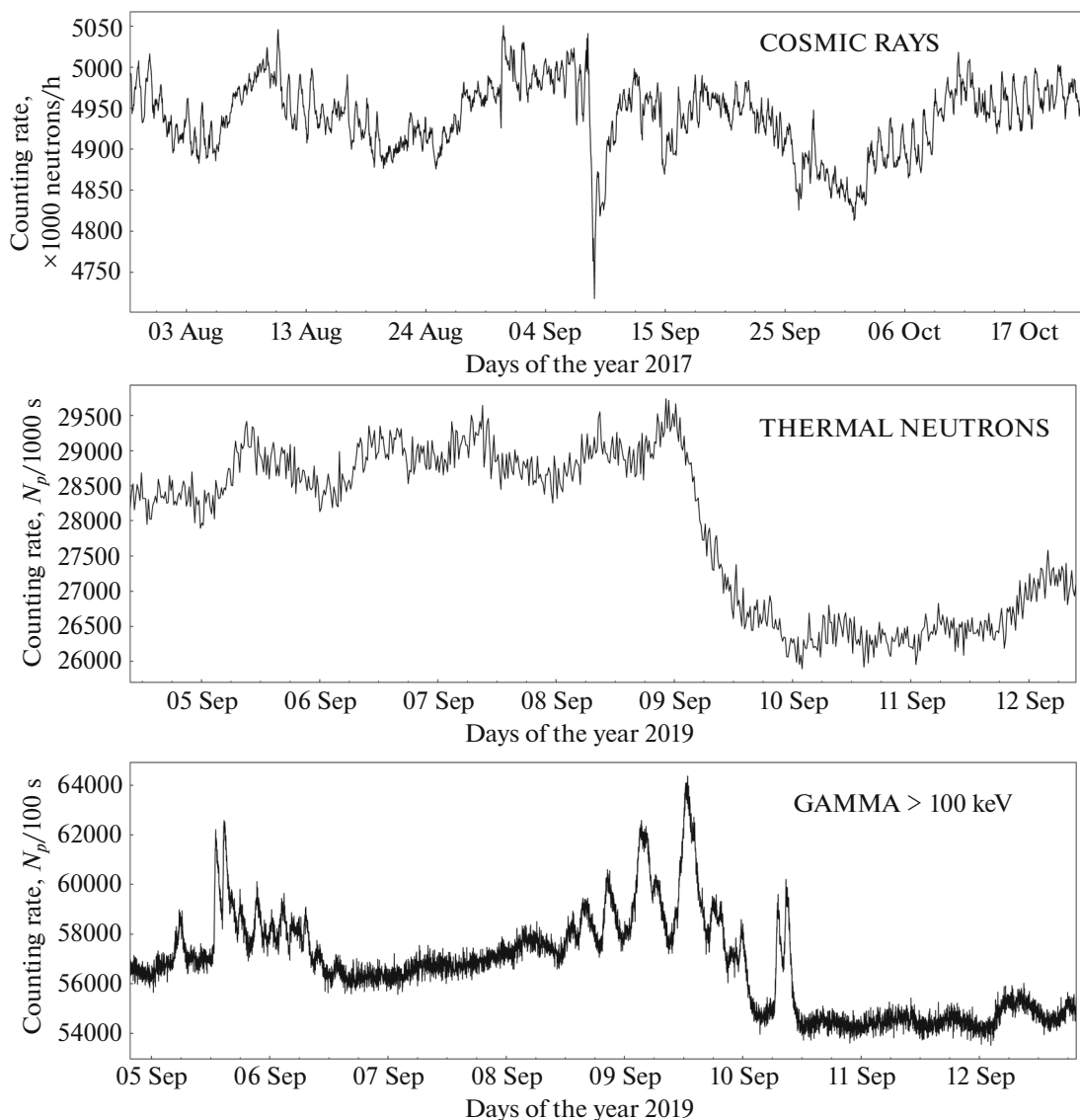


**Fig. 1.** Examples of the radiation monitoring data obtained at the Tien Shan experimental complex. Top frame: footprint of the big Forbush effect on September 8, 2017 in the time history of the counting rate at the Tien Shan neutron monitor. Middle and bottom frames: the records of radiation background in the surrounding environment made by the neutron and gamma detectors over a week duration in September 2019. Vertical axes are graduated in the units of signals number  $N_p$  normalized to the time span of a single measurement.

### 3. INVESTIGATION OF LIGHTNING PROCESSES IN THUNDERCLOUDS

The Tien Shan mountain station is a convenient site for studying the processes of atmospheric electricity, since during the whole summer season the thunderstorm clouds move here at a low altitude above the ground surface, starting from distance of  $\sim(50-100)$  m only. This circumstance permits a fairly effective registration of the radiation from lightning discharges using a variety of detectors which can be installed both on the territory of the station itself, and on the slopes of surrounding mountains. In addition, the availability of the cosmic ray particles detectors at the station makes it possible to study

the role of cosmic rays and extensive air showers in the process of lightning initiation which presently remains under active discussion. Correspondingly, a detector system “Thunderstorm” has been created at the station in early 2000s as a part of its multipurpose experimental complex, and has been since remaining under constant stepwise development.

The experimental system “Thunderstorm” includes the particles detectors for registering electrons, gamma-rays, neutrons, as well as the receivers of lightning emission in the different wave ranges of the electromagnetic spectrum, and the sensors of the local electric field and nearby atmospheric discharges. In the technical design of all detector devices the

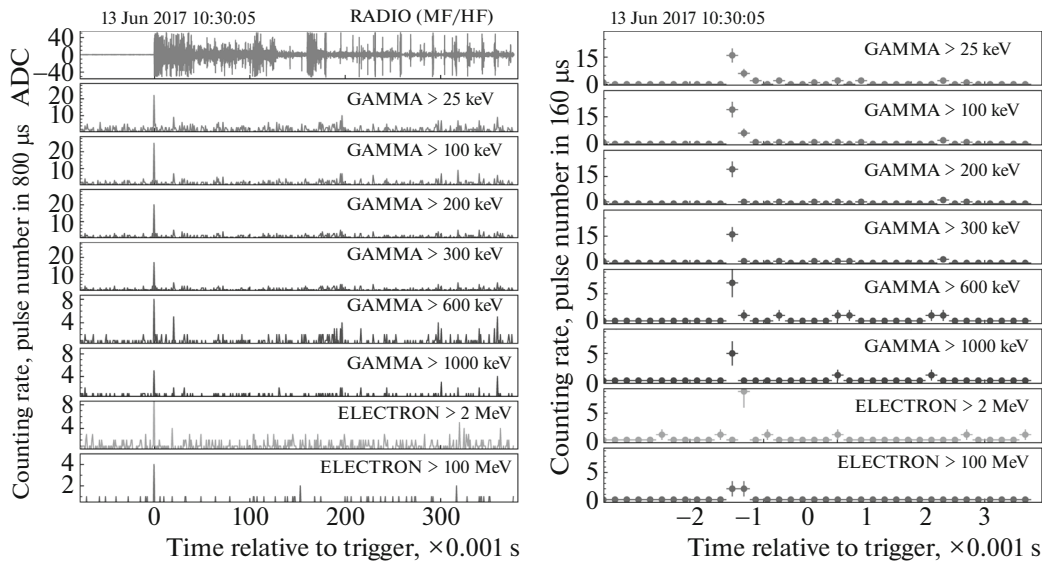


**Fig. 2.** Short-time burst of the intensity of accelerated electrons and gamma-rays at a lightning initiation moment detected at distance  $\sim 50$  m from the discharge core. The time resolution of data series is  $800 \mu\text{s}$  in the left plot, and  $160 \mu\text{s}$  in the right; zero point of abscissa axes corresponds to the initiation moment of lightning discharge.

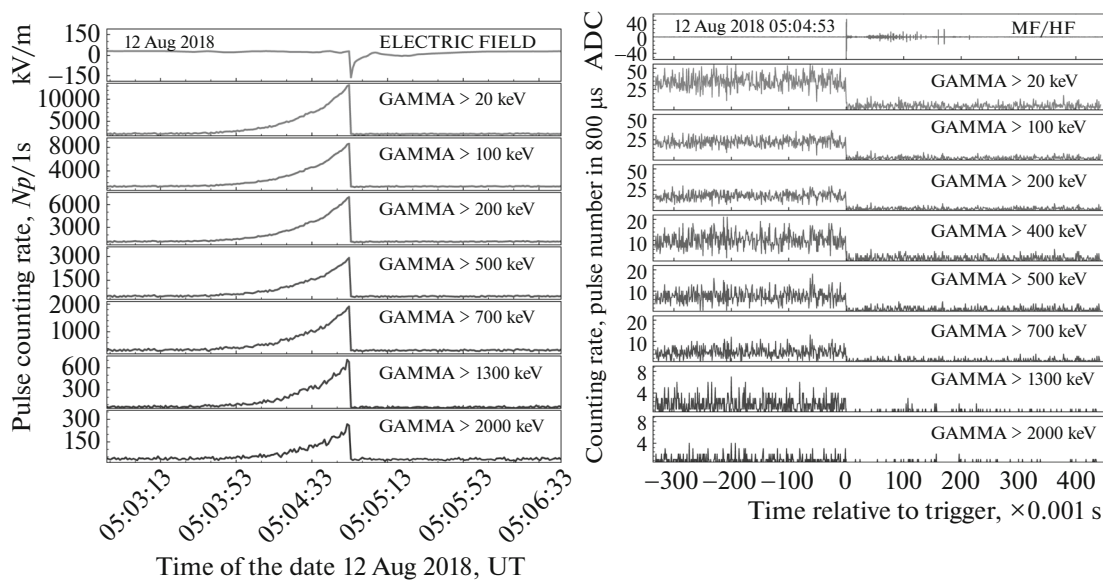


**Fig. 3.** The thunderstorm gamma enhancement event as seen in depth of thundercloud. Left: the monitoring data of gamma-ray intensity with different energy thresholds. Right: the counting rate of gamma-radiation around the moment of lightning discharge which has terminated the TGE. Zero point of abscissa axis corresponds to the moment of the lightning. Time resolution of the data series is 1 s in the left plot, and  $800 \mu\text{s}$  in the right.

possibility was especially foreseen of stable operation in thunderstorm conditions, and under intensive electromagnetic interference from close lightnings.

In particular, for the purpose of lightning investigation a special high-altitude detector point was created at a mountain top,  $\sim 450$  m above the average level of the station. The electronic equipment placed there is used for direct registration of accelerated electrons and gamma-rays in the depth of thunder-

cloud, at a minimum distance from the spatial region of lightning development which frequently occurs to be of the order of tens of meters only. The proximity to lightning core makes it possible to avoid significant absorption and distortion of energy spectra of generated radiations on their way to the detector [16]. Several examples of physical results obtained in thunderstorm time at the high-altitude detector point are presented in Figs. 2–4.

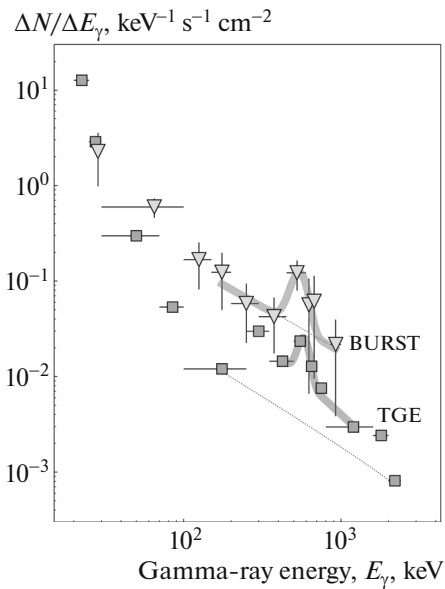


**Fig. 4.** The differential energy spectra of gamma-radiation in the two events from Figs. 2 and 3.

In Fig. 2 the time series of the counting rate in the gamma-ray and electron detectors are shown which were measured at the high altitude detector point at initiation moment of a close lightning discharge. The registration of radiation fluxes at that time was made with several energy thresholds, of  $\sim 1$  MeV and  $\sim (100\text{--}200)$  MeV for electrons, and from  $\sim 20$  keV up to  $\sim 1$  MeV for gamma-rays. The linear distance from the detector point to the discharge region in that case was  $\sim (50\text{--}100)$  m, as estimated by the delay of thunder sound relative to the lightning. The precise time profile of lightning development can be traced by synchronous record of the (1–30) MHz (MF/HF) radio-emission in one of the panels of the figure.

It is seen a short prominent intensity outburst in all signal series of Fig. 2 which coincides with the moment of lightning initiation and has a typical duration  $\lesssim (0.1\text{--}0.3)$  ms. Because of the presence at that moment of a distinct imprint of high-energy electrons in corresponding panels of the figure this burst can be interpreted as direct detection event of an electron—photon avalanche which has given start to development of the lightning discharge [22].

Another kind of atmospheric electricity phenomena is illustrated by Fig. 3 where an event of thunderstorm ground enhancement type (TGE) is presented as it was detected at the high altitude point deeply immersed into a thundercloud. Generally, the events of such type are caused by passage of a quasi-stable active region of thundercloud with the processes of charge separation actively going on [23, 24]. In contrast to the burst event above, the total duration of radiation rise in this case lasted up to several

minutes and terminated at the moment 05:04:53 UT by a lightning discharge which occurred at distance  $\sim 100$  m from the detector point.

At last, Fig. 4 demonstrates the differential energy spectra of gamma-radiation calculated by the counting rate data of both considered events. It is seen there a peak around the gamma-ray energy  $\sim 500$  keV which can be interpreted as a positron annihilation line. The emergence of positrons in thunderclouds is a cornerstone feature of some models suggested up to date for explanation of the process of lightning development [25–27].

Besides hard radiations, by study of the processes related to atmospheric electricity it is of interest also the fine temporal structure of electric discharges which can be revealed through detection of the different kinds of lightning emission. For the purpose, there were installed at the Tien Shan station the optical detectors sensitive in the ultraviolet, (200–400) nm, and near infrared, (600–800) nm, wave ranges of the electromagnetic spectrum [15], as well as the receivers of radio-emission from close atmospheric discharges in the MF/HF frequency range of (1–30) MHz [14, 28]. Another experiment of similar type presently running at the Tien Shan station is connected with detection of the short-time electromagnetic pulses (“atmospherics”) generated by far thunderstorms in the VLF range of (1–10) kHz, and propagating to large distances over the global earth-ionosphere waveguide. During thunderstorms all these sensors operate synchronously to ensure multi-channel registration of the temporal profiles of lightning development with time resolution from 20 to  $800\ \mu\text{s}$ . Some examples of such records are shown in the plots of Fig. 5.

A most typical event is presented in the top left plot of Fig. 5. It is seen there that in this case the lightning process was accompanied by an abrupt jump of the local electric field with absolute amplitude of  $\sim 100$  kV/m, and with a change of field polarity. The lightning itself had characteristic stepped structure consisting of a multitude of narrow peaks separated by the deep gaps with a several orders of magnitude smaller emission. The radiation peaks detected simultaneously in the ultraviolet and infrared channels, as usual, had comparable amplitudes. The whole duration of the discharge in the considered case was of  $\sim 1$  s, but relaxation of the electric field to zero level afterwards took an order of magnitude longer time. The sound of thunder arrived to the detector point after a  $\sim 3$  s time delay, so the distance to discharge region in this particular event was of about 1 km.

Detailed investigation of the time series of lightning emission permitted to reveal the atmospheric discharges with some peculiarities in their development. An example of such events is presented in

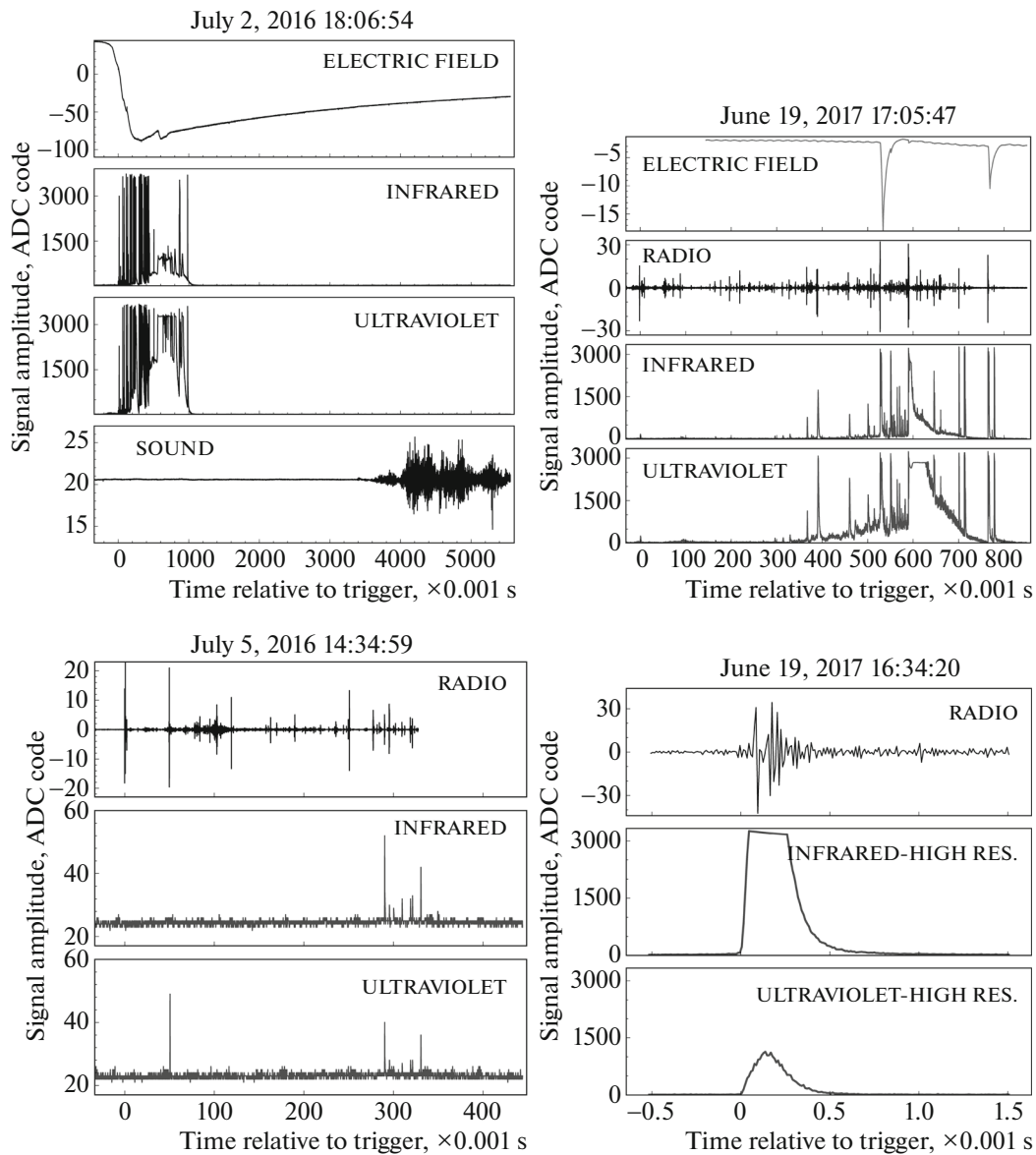


**Fig. 5.** Exemplary time series of lightning emission detected in the different wave ranges of the electromagnetic spectrum. Zero point of time axis in all plots corresponds to beginning of lightning discharge.

the top right plot of Fig. 5. In this case the electric discharge itself lasted over  $\approx 0.8$  s, as it can be traced by the time history of its (1–30) MHz signal which is shown in the RADIO panel of the plot. In contrary, both in the ultraviolet and infrared wave ranges the lightning started to be detectable only at the moment of (300–350) ms after the starting point of the discharge, so its whole initial part remained “dark,” i.e., without any visible emission. Similar behavior demonstrates the event shown in the bottom left frame, which additionally had a peculiar energy distribution in its spectrum: as it is seen in the plot, an “ultraviolet” peak at the moment of  $\approx 50$  ms does not have any corresponding counterpart in the infrared wavelength range. This feature cannot be any

artifact of incorrect detector operation at that time since the group of emission peaks at  $\approx 300$  ms in the same distribution has an ordinary relation of signal amplitudes between the two wave range channels. An opposite inequality of signal amplitudes demonstrates the event in the bottom right plot of Fig. 5, where the amplitude of signal detected in the infrared channel is essentially higher than that of the ultraviolet peak. As well, the “red flash” event in bottom right is illustrative case of a specific class of extremely short electric discharges with total duration  $\lesssim 1$  ms, existence of which was revealed in the experiments running at the Tien Shan mountain station.



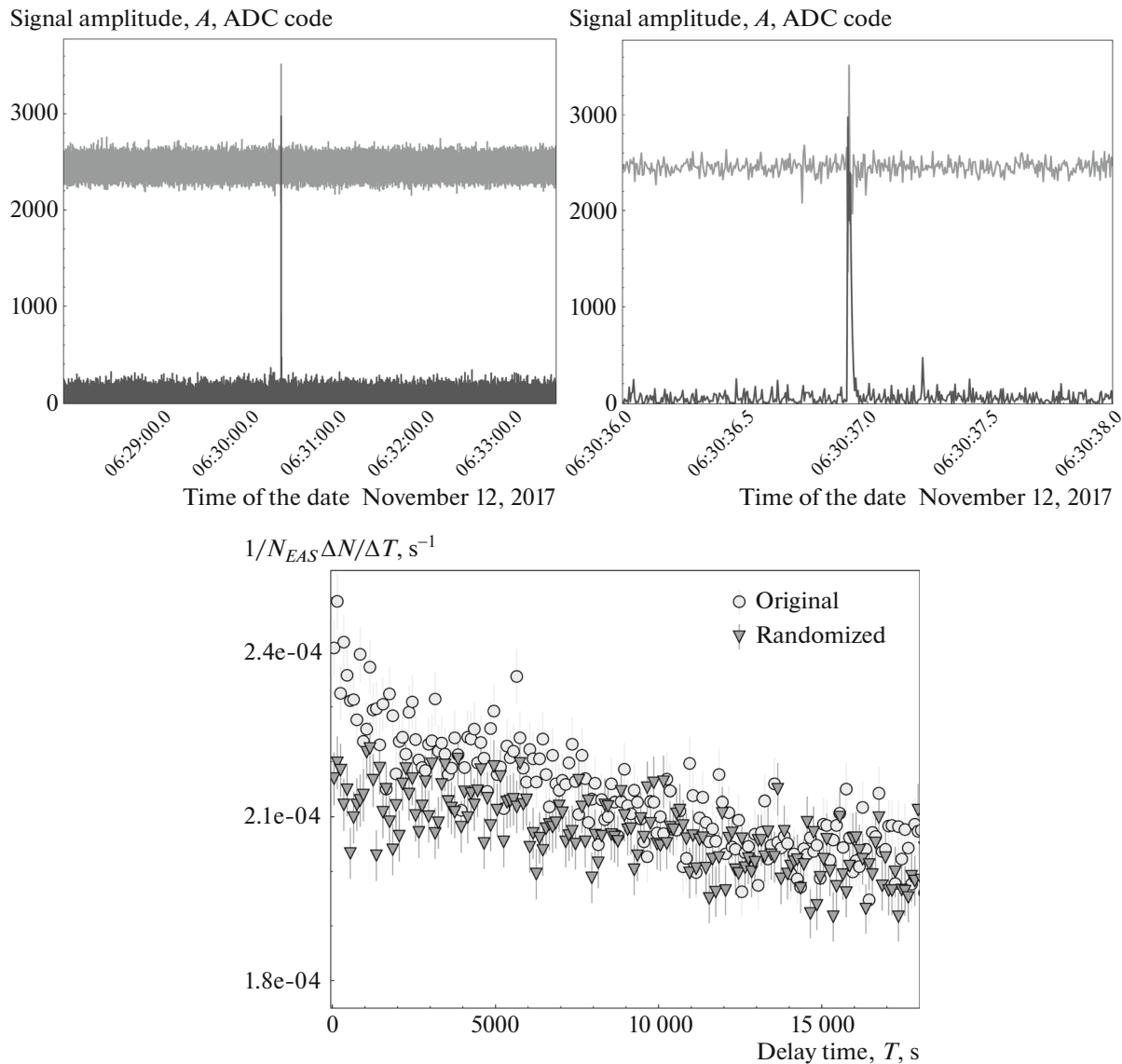


**Fig. 6.** Top: typical sporadic outburst of the intensity of microphone signal (an “acoustic event”). Upper curve in the plots corresponds to direct microphone signal, the lower one is its low-frequency envelope. The time axis in the right plot is zoomed around the moment of the event. Bottom: the distribution of time delays between the powerful extensive air showers and succeeding acoustic events (circles), and between the showers and the random time moments (triangles).

#### 4. SEISMOLOGICAL STUDIES

In recent years the works were initiated at the Tien Shan station on a long-term monitoring of a variety of diverse geophysical parameters. This line of research includes the measurement of the Doppler frequency shift at ionosphere sounding, registration of low-frequency electromagnetic pulses in the frequency ranges of (1–10) kHz and (1–100) Hz, monitoring of telluric currents, as well as continuous intensity measurements of the gamma-ray and neutron background, of acoustic signals, and of the level of subsoil waters by a special set of detectors installed in a deep borehole located at the territory of the station. The

main final goal of these measurements is using their results for the purpose of seismological prognosis.

In particular, an experiment is presently running at the station on the search for correlations between the acoustic signals of seismic origin and the passage events of energetic particles of the penetrating component of cosmic rays. As such, the muons with the energy of about 1 TeV and above can be considered which are capable to penetrate into the earth’s crust up to the depth of the order of several kilometers. Calculations show that the ionization created by such particles could serve as a trigger for release of elastic deformation energy accumulated at the edges of a deep lithosphere fault situated under the

surface of the Tien Shan station [29, 30]. This process leads to creation of micro-cracks in the lithosphere material and generation of elastic vibrations in the acoustic frequency range. The latter propagate over the earth's crust in the form of a sound wave and can be detected near the surface of the ground by sensitive microphones. It is important that the events of muon passage supposedly preceding the microphone signal can be effectively traced by the means of appropriate detectors located at the Tien Shan station, so the discussed effect, if it would be confirmed by experiment, could be a source of real time information on current conditions at the depth of lithosphere.

The state of the art of an experiment aimed to testing this hypothesis is illustrated by Fig. 6. In both top frames of this figure a fragment of the time history of microphone signal is plotted which was uninterruptedly recorded in the borehole of the Tien Shan station during the date of November 12, 2017. There are two curves in these plots: a direct record of the analog signal from the microphone output (above), and its low-frequency envelope obtained by feeding this signal to a low-pass analog filter (below). Over a generally smooth background in both these records a short standalone intensity outburst is seen with duration of several tenths of second and amplitude an order of magnitude above the standard deviation level of background fluctuations. As it turns out, such phenomena, which further on will be referenced to as "acoustic events," are frequently met among the records of microphone signal. Their daily counts variate sporadically in a wide range of values, starting from (1–5) and up to several hundreds of events per a day, and they do not demonstrate any obvious correlation with daytime, seasonal, or weather conditions, nor with the periods of human activity.

In supposition that the acoustic events could be an observable effect of elastic vibrations provoked by passage of penetrative cosmic ray particles at the depth of lithosphere and propagating over the earth's crust, it was made a statistical analysis of the time delay distribution between the passage moments of extensive air showers (EAS) and succeeding acoustic events. In this study the EAS were considered which had been created by the primary cosmic ray particles with the energy above 1 PeV, as defined by the Tien Shan installation of the shower particles detectors [1]. It is known that in the core region of such EAS the muons with TeV scale energy can be concentrated which stem from interaction of high-energy cosmic ray particles at the early development stage of atmospheric cascade. A distribution of such type is presented, by circles, in the bottom plot of Fig. 6.

An experimental distribution of time delays between the EAS and succeeding acoustic events in the plot is compared against an analogous one which

was built for the delays between the EAS and random time moments. It is seen that in the range of time intervals below (1000–2000) s there exists a statistically significant excess of the probability with which such delays were met between the EAS and acoustic pulses above the fully random distribution. This is an experimental evidence in favor of the hypothesis on possibility of induced generation of acoustic signals of seismological origin under the triggering influence of cosmic ray muons.

## 5. CONCLUSIONS

The scientific complex of experimental installations created at the Tien Shan mountain station of LPI opens opportunity to carry out researches in a wide range of problems connected with different Earth sciences. Some exemplary results presented in the paper demonstrate effectiveness of the investigation methods developed at the station for the purpose.

## FUNDING

This research has been funded by the Science Committee of the Ministry of Education and Science of the Republic of Kazakhstan, grant nos. AP08855916, AP09260262, and AP09258896.

## REFERENCES

1. A. P. Chubenko, A. L. Shepetov, V. P. Antonova, A. S. Borisov, O. D. Dalkarov, O. N. Kryakunova, K. M. Mukashev, R. A. Mukhamedshin, R. A. Nam, N. F. Nikolaevsky, V. P. Pavlyuchenko, V. V. Piscal, V. S. Puhkov, V. A. Ryabov, T. Kh. Sadykov, N. O. Saduev, et al., *Nucl. Instrum. Methods Phys. Res., Sect. A* **832**, 158 (2016); arXiv:1912.13356.
2. A. V. Gurevich, A. M. Almenova, V. P. Antonova, A. P. Chubenko, A. N. Karashtin, O. N. Kryakunova, V. Yu. Lutsenko, G. G. Mitko, V. V. Piscal, M. O. Ptitsyn, V. A. Ryabov, N. M. Salikhov, A. L. Shepetov, Y. V. Shlyugaev, W. M. Thu, L. I. Vildanova, et al., *Phys. Rev. D* **94**, 023003 (2016).
3. A. G. Zusanovich, O. N. Kryakunova, and A. L. Shepetov, *Adv. Space Res.* **44**, 1194 (2009).
4. A. Shepetov, A. Chubenko, B. Iskhakov, O. Kryakunova, O. Kalikulov, S. Mamina, K. Mukashev, V. Piscal, V. Ryabov, N. Saduev, T. Sadykov, N. Salikhov, E. Tautaev, L. Vil'danova, and V. Zhukov, *Eur. Phys. J. Plus* **135**, 96 (2020); arXiv:1912.13173.
5. A. P. Chubenko, V. P. Antonova, S. V. Kryukov, V. V. Piscal, M. O. Ptitsyn, A. L. Shepetov, L. I. Vildanova, K. P. Zybin, and A. V. Gurevich, *Phys. Lett. A* **275**, 90 (2000).
6. A. P. Chubenko, I. V. Amurina, V. P. Antonova, S. V. Kryukov, K. M. Mukhashev, R. A. Nam, N. M. Nesterova, V. V. Oskomov, V. V. Piscal, M. O. Ptitsyn, T. Kh. Sadykov, A. L. Shepetov, L. I. Vildanova, K. P. Zybin, and A. V. Gurevich, *Phys. Lett. A* **309**, 90 (2003).



7. A. V. Gurevich, A. N. Karashtin, A. P. Chubenko, L. M. Dunan, V. A. Ryabov, A. L. Shepetov, V. P. Antonova, S. V. Kryukov, V. V. Piscal, M. O. Ptitsyn, Yu. V. Shlyugaev, and K. P. Zybin, *Phys. Lett. A* **325**, 389 (2004).
8. A. P. Chubenko, A. N. Karashtin, V. A. Ryabov, A. L. Shepetov, V. P. Antonova, S. V. Kryukov, G. G. Mitko, A. S. Naumov, V. P. Pavlyuchenko, M. O. Ptitsyn, S. Ya. Shalamova, Yu. V. Shlyugaev, L. I. Vildanova, K. P. Zybin, and A. V. Gurevich, *Phys. Lett. A* **373**, 2953 (2009).
9. A. V. Gurevich, A. N. Karashtin, V. A. Ryabov, A. P. Chubenko, and A. L. Shepetov, *Phys. Usp.* **52**, 735 (2009).
10. A. V. Gurevich, G. G. Mitko, V. P. Antonova, A. P. Chubenko, A. N. Karashtin, S. V. Kryukov, A. S. Naumov, V. P. Pavljuchenko, M. O. Ptitsyn, V. A. Ryabov, S. Ya. Shalamova, A. L. Shepetov, Yu. V. Shlyugaev, L. I. Vildanova, and K. P. Zybin, *Phys. Lett. A* **373**, 3550 (2009).
11. A. V. Gurevich, A. P. Chubenko, A. N. Karashtin, G. G. Mitko, A. S. Naumov, M. O. Ptitsyn, V. A. Ryabov, A. L. Shepetov, Yu. V. Shlyugaev, L. I. Vildanova, and K. P. Zybin, *Phys. Lett. A* **375**, 1619 (2011).
12. A. V. Gurevich, V. P. Antonova, A. P. Chubenko, A. N. Karashtin, G. G. Mitko, M. O. Ptitsyn, V. A. Ryabov, A. L. Shepetov, Yu. V. Shlyugaev, L. I. Vildanova, and K. P. Zybin, *Phys. Rev. Lett.* **108**, 125001 (2012).
13. A. V. Gurevich, V. P. Antonova, A. P. Chubenko, A. N. Karashtin, O. N. Kryakunova, V. Yu. Lutsenko, G. G. Mitko, V. V. Piscal, M. O. Ptitsyn, V. A. Ryabov, A. L. Shepetov, Yu. V. Shlyugaev, W. M. Thu, L. I. Vildanova, and K. P. Zybin, *Atm. Res.* **164–165**, 339 (2015).
14. A. V. Gurevich, V. P. Antonova, A. P. Chubenko, A. N. Karashtin, G. G. Mitko, M. O. Ptitsyn, V. A. Ryabov, A. L. Shepetov, Yu. V. Shlyugaev, W. M. Thu, L. I. Vildanova, and K. P. Zybin, *Phys. Rev. Lett.* **111**, 165001 (2013).
15. A. V. Gurevich, G. K. Garipov, A. M. Almenova, V. P. Antonova, A. P. Chubenko, O. A. Kalikulov, A. N. Karashtin, O. N. Kryakunova, V. Yu. Lutsenko, G. G. Mitko, K. M. Mukashev, R. A. Nam, N. F. Nikolayevsky, V. I. Osedlo, M. I. Panasyuk, V. V. Piscal, et al., *Atm. Res.* **211**, 73 (2018).
16. A. Shepetov, V. Antonova, O. Kalikulov, O. Kryakunova, A. Karashtin, V. Lutsenko, S. Mamina, K. Mukashev, V. Piscal, V. Ryabov, T. Sadykov, N. Saduyev, N. Salikhov, Yu. Shlyugaev, L. Vildanova, V. Zhukov, and A. Gurevich, *Atm. Res.* **248**, 105266 (2021); arXiv: 2009.07307.
17. N. Salikhov, A. Shepetov, A. Chubenko, O. Kryakunova, and G. Pak, arXiv: 1301.6965.
18. K. M. Mukashev, T. K. Sadykov, V. A. Ryabov, A. L. Shepetov, G. Y. Khachikyan, N. M. Salikhov, A. D. Muradov, O. A. Novolodskaya, V. V. Zhukov, and A. K. Argynova, *Acta Geophys.* **67**, 1241 (2019).
19. The Tien-Shan Mountain Station's Database, 2006–2021. <http://www.tien-shan.org>.
20. H. Carmichael and C. J. Hatton, *Can. J. Phys.* **42**, 2443 (1964).
21. C. J. Hatton and E. V. Tomlinson, *Nuovo Cim.* **53**, 63 (1968).
22. A. V. Gurevich, G. A. Milikh, and R. Roussel-Dupré, *Phys. Lett. A* **165**, 463 (1992).
23. T. Torii, T. Sugita, M. Kamogawa, Y. Watanabe, and K. Kusunoki, *Geophys. Res. Lett.* **38**, L24801 (2011).
24. A. Chilingarian, T. Karapetyan, and L. Melkumyan, *Adv. Space Res.* **52**, 1178 (2013).
25. J. R. Dwyer, *J. Geophys. Res.* **115**, A00E14 (2010).
26. T. Enoto, Y. Wada, Y. Furuta, K. Nakazawa, T. Yuasa, K. Okuda, K. Makishima, M. Sato, Y. Sato, T. Nakano, D. Umemoto, and H. Tsuchiya, *Nature (London, U.K.)* **551**, 481 (2017).
27. L. P. Babich, *Phys. Usp.* **62**, 976 (2019).
28. A. N. Karashtin, Y. V. Shlyugaev, and A. V. Gurevich, *Radiophys. Quantum Electron.* **48**, 711 (2005).
29. G. A. Gusev, V. V. Zhukov, G. I. Merzon, G. G. Mitko, V. A. Ryabov, A. V. Stepanov, V. A. Chechin, A. P. Chubenko, and A. L. Shchepetov, *Bull. Lebedev Phys. Inst.* **38**, 374 (2011).
30. L. I. Vildanova, G. A. Gusev, V. V. Zhukov, G. I. Merzon, G. G. Mitko, A. S. Naumov, V. A. Ryabov, A. V. Stepanov, V. A. Chechin, A. P. Chubenko, and A. L. Shchepetov, *Bull. Lebedev Phys. Inst.* **40**, 74 (2013).